https://doi.org/10.5194/egusphere-2024-107
Preprint. Discussion started: 30 January 2024

Soil organic carbon mineralization is controlled by the application dose of exogenous organic matter

Orly Mendoza [1], Stefaan De Neve [1], Heleen Deroo [1], Haichao Li [1], Astrid Françoys [1,2], Steven Sleutel [1]

[1] Department of Environment, Ghent University, Coupure Links 653, 9000 Ghent, Belgium
[2] Isotope Bioscience Laboratory, Department of Green Chemistry and Technology, Ghent University, Coupure Links 653, 9000 Ghent, Belgium

Correspondence to: Orly Mendoza (mendozaorly@gmail.com)

Abstract. Substantial input of exogenous organic matter (EOM) may be required to offset the projected decline in soil organic carbon (SOC) stocks in croplands caused by global warming. However, information on the effectivity of EOM application dose in preserving SOC stocks is surprisingly limited. Therefore, we set up a 90-day incubation experiment with large soil volumes (sandy loam and silt loam) to compare the mineralization of EOM (^{13}C-labelled ryegrass) and SOC as a function of three EOM application doses (0.5, 1.5, and 5 g dry matter kg^{-1} soil). In the sandy loam soil, the percentage of mineralized EOM was not affected by EOM dose, while SOC mineralization increased proportionally with increasing EOM dose (+49.6 mg C per g EOM). In the silt loam soil, the percentage of mineralized EOM decreased somewhat with increasing dose, while SOC mineralization increased at a higher rate than in the sandy loam soil (+117.2 mg C per g EOM). In both textured soils, increasing EOM dose possibly supplied energy for microbial growth and enzyme production, which in turn stimulated mineralization of native SOC (i.e. co-metabolism). Higher soil macroporosity at higher EOM doses in the silt loam soil could have contributed to sustaining aerobic conditions (indicated by soil Eh) and promoting SOC priming as shown by positive relationships between pore neck size classes 43–60, 60–100 and >300 µm and SOC priming, suggesting a new mechanism for understanding SOC priming. In sum, this experiment and our previous research suggest that EOM mineralization is mostly independent of EOM dose, but EOM dose modulates mineralization of native SOC. These findings tentatively indicate that using larger EOM doses could help preserve more of added EOM-C in silt loam soils, but longer-term confirmation in the field will firstly be required before we could draw any conclusion for soil C management.

1 Introduction

Small changes in global carbon (C) stocks can cause significant changes in climate (Smith et al., 2020). Croplands are a potential global C sink because of their lower soil organic carbon (SOC) content relative to that of the corresponding native ecosystems (Paustian et al., 1997). Zomer et al. (2017) estimated that croplands could potentially sequester 0.90–1.85 Gt C year^{-1}, representing a substantial portion (i.e. 26–53 %) of the 4p1000 initiative target (3.4 Gt C year^{-1}) that aims at offsetting most of the annual increase in atmospheric CO_2 (15.8 Gt CO_2 year^{-1} or 4.3 Gt C year^{-1}) (Paustian et al., 2019). To preserve SOC stocks and soil fertility, most agricultural systems rely on the application of exogenous organic matter (EOM) to the soil, usually as crop residue or animal manure. Depending on its composition and dose, EOM contributes significantly to the overall soil C balance, which can be derived using soil C balance calculations or simulation model runs. In the frequently used Hénin and Dupuis mathematical model, a certain fixed fraction of EOM is assumed to 'contribute' to SOC (Hénin and Dupuis, 1945). In both empirical and more complex process-based SOC simulation models, EOM degradability is primarily determined by its quality, soil texture, and soil environmental parameters, such as temperature, moisture content, and availability of N. However, the EOM dose (amount of C added per kg soil or per m^2) has supposedly little or no impact on its mineralization rate or on the mineralization rate of SOC in SOC models. For example, the Roth-C model (Jenkinson et al., 2008; Powlson et al., 2013) simulates an unrestricted response of C

https://doi.org/10.5194/egusphere-2024-107
Preprint. Discussion started: 30 January 2024

mineralization to C concentration. The DNDC model simulates several anaerobic processes via Michaelis-Menten kinetics (Li et al., 1997), i.e. with a feedback to exogenous organic carbon (EOC) dosage, but again the aerobic mineralization of C follows first-order kinetics.

Nevertheless, several reasons have been provided for feedback between the EOM dose and its decomposition in soil. First, the fate of OM in soil can be controlled by its accessibility to decomposers (Dungait et al., 2012; Lehmann et al., 2020). Thus, larger soil EOM quantities may promote closer contact with decomposers and positive impacts on EOM and SOC mineralization. Don et al. (2013) demonstrated that total SOC was more readily mineralized when the added EOM (compost) was concentrated as opposed to when it was dispersed in soil. Kuzyakov and Domanski (2000) also argued that the local disproportional growth of microbial biomass and stimulation of its activity with EOM dose may have positive effects on EOM and SOC decomposition via co-metabolism or other SOC priming mechanisms. However, negative SOC priming might also occur if, for instance, higher stimulated heterotrophic activity leads to local depletion of O_2 during decomposition, slowing down further EOM mineralization. Second, stimulated microbial activity at higher EOM doses might indirectly modulate soil microbial activity by controlling soil structure development. De Gryze et al. (2005) reported that increasing the doses of wheat residue led to a proportional formation of soil aggregates. Furthermore, Shahbaz et al. (2017a) concluded that adding a higher dose of wheat residue (1.40 vs. 5.04 g dry matter kg^{-1}) stimulated macroaggregate formation, resulting in positive priming of SOC in a silt loam soil. Using the same soil but higher wheat residue doses (5.4 and 10.8 g kg^{-1} soil vs. 1.40 and 5.04 g kg^{-1} soil), Shahbaz et al. (2017b) also reported that SOC priming diminished at high dose. Similarly, Mendoza et al. (2022a) observed that increasing EOM (ground maize straw and ryegrass) doses stimulated soil macroporosity but did not affect EOM mineralization. Such control of soil structure and potential feedback to EOM and SOC mineralization can be soil specific. Increasing the application dose of ^{13}C-labelled ryegrass promoted the formation of meso- and macropores, and their volume percentages correlated positively with the magnitude of positive SOC priming effects in a sandy loam but not in a silt loam soil (Mendoza et al., 2022b). Finally, adding relatively N-poor EOM at a higher dosage can adversely impact its degradation due to the temporal shortage of mineral N in soil for microbial decomposers.

The conclusions of the above-mentioned studies, focusing on C mineralization in response to the application dose, were mostly based on simplified soil systems. Despite the diverse chemical complexity encountered in real conditions, laboratory experiments studying dosage effects on C mineralization are often limited by the use of single chemical compounds, such as glucose (Blagodatskaya et al., 2007; Schneckenberger et al., 2008; Liu et al., 2017). More complex plant-derived substrates were finely ground and mixed in soil, such as <2 mm wheat residue (Shahbaz et al., 2017a, b), ground maize straw particles (Mendoza et al., 2022a), and ±2 cm chopped pieces of ryegrass (Mendoza et al., 2022b). Such finer EOM sources likely decompose differently in laboratory than in field conditions because of the large surface area of the residue in contact with the soil (Garnier et al., 2008); on the other hand, a potentially stronger interaction with the soil mineral phase may protect OM from decomposition. Both phenomena may render the EOM dosage responses from laboratory incubations unrepresentative of OM degradation in the field. Under field conditions, the much larger pieces of crop residue probably constitute C hotspots with a more locally confined but stronger impact on soil structure and biological soil processes. Moreover, at such C hotspots, oxygen shortages may impede aerobic soil C mineralization. Such responses have been largely overlooked when interpreting soil C mineralization data (Keiluweit et al., 2017), and soil structure should also be kept as intact as possible to account for those aspects.

In this study, we aimed to quantify the effect of EOM application dose on EOM and SOC mineralization in an incubation experiment with large soil cores using large pieces of ^{13}C-labelled ryegrass residue. We hypothesized that the mineralized percentage of added EOM (further referred to as relative EOM mineralization) would increase with increasing application

https://doi.org/10.5194/egusphere-2024-107
Preprint. Discussion started: 30 January 2024

dose. To gain insight into the potential indirect control of EOM dose on its mineralization via the mediation of soil aeration and structure, the effects of EOM dosage on soil redox potential and pore neck size distribution were assessed. The experiment was performed in both sandy loam and silt loam soils. We expected that in finer-textured soil, O_2 provision would more readily limit EOM mineralization at higher EOM doses. We also hypothesized that SOC mineralization would be stimulated as a larger EOM application dose would lead to SOC priming, which can be linked to the classical co-metabolism mechanism and to promoted soil aeration because of a developed soil structure.

2 Materials and methods

2.1 Soils and labelled ^{13}C ryegrass used in the incubation experiments

A soil incubation experiment was set up with different EOM doses and soil textures to investigate their interactive effect on EOM-C mineralization. Two topsoils were selected with contrasting soil texture, i.e. sandy loam and silt loam, but with similar SOC content, C:N ratio (10 and 9, respectively), and $\delta^{13}C$ (Table 1). These soils were sampled at a depth of approximately 5 to 20 cm at the Institute for Agricultural Research in Melle, Belgium and at a nearby farmer's field in Oosterzele, East Flanders, Belgium.

^{13}C-pulse-labelled ryegrass was used as the model EOM for a reliable discrimination of EOM and SOC mineralization based on $^{13/12}C$-resolved soil CO_2 efflux measurements. ^{13}C-pulse-labelling was performed at the Ghent University experimental farm in Bottelare, Belgium by weekly exposure of initially pruned ryegrass (*Lolium perenne* L.) for two months to a temporarily $^{13}CO_2$-enriched atmosphere inside Plexiglas labelling chambers. These $^{13}CO_2$ flushes were obtained by reacting 0.3 M sodium bicarbonate-^{13}C ($NaH^{13}CO_3$ 98 atom % ^{13}C) with 1 M hydrochloric acid (HCl) inside the chambers that were outfitted with fans, sealed on the ground, and closed overnight on top of 0.8×0.8 m microplots in the ryegrass field. After 8 weeks, ryegrass was cut with a sickle and had a resulting $\delta^{13}C$ of +51±5.4 ‰ (n = 6), C content of 439.3±5.4 g kg^{-1}, and C:N of 10±0.5. Harvested and dried ^{13}C-labelled ryegrass from young and more senescent plant parts differed by only 3.8‰, demonstrating that the material was uniformly ^{13}C labelled.

Table 1. Physicochemical characteristics of the two selected topsoils used in the soil incubation experiment. Averages of three replicates with standard errors are shown for pH, and measurements of two replicates are shown for Al_{ox}, Fe_{ox}, P, Ca, K, and Mg.

Soil characteristic	Sandy loam	Silt loam
Sand (%)	60.2	13.3
Silt (%)	26.9	67.0
Clay (%)	12.9	19.7
SOC (g kg^{-1})	14.4±0.4	14.9±0.3
$\delta^{13}C$ (‰)	−27.72	−25.11
$pH_{(H2O)}$[a]	6.4±0.0	7.4±0.0
Al_{ox} (mg kg^{-1})[b]	1199.4 – 1172.7	679.7 – 693.7
Fe_{ox} (mg kg^{-1})[b]	3221.0 – 3183.0	4280.5 – 4302.0
P (mg kg^{-1})[c]	85.7 – 87.8	325.6 – 329.0
Ca (mg kg^{-1})[c]	954.5 – 953.8	2429.2 – 2488.0
K (mg kg^{-1})[c]	148.0 – 147.5	320.5 – 327.2
Mg (mg kg^{-1})[c]	125.2 – 125.0	142.4 – 146.3

[a]$pH_{(H2O)}$ was obtained by inserting a glass pH electrode in 1:6.25 soil-H_2O mixture. [b]NH_4-oxalate extraction and detection using inductively coupled plasma optical emission spectroscopy (ICP-OES). [c]NH_4–acetate-EDTA extraction and ICP-OES analysis.

https://doi.org/10.5194/egusphere-2024-107
Preprint. Discussion started: 30 January 2024

2.2 Soil incubation and experimental design

The soils collected from the field were kept moistened and sieved through a 10 mm mesh to keep initial soil structure and aggregation as intact as possible. Moist soil directly limited the disruption of the original soil structure (macro-aggregation) during sieving. The collected air-dried ryegrass biomass (no further refinement after harvesting) was mixed into 7.96 kg of moist sandy loam soil and 7.78 kg of moist silt loam soil at application doses of 0.5, 1.5 and 5 g dry matter kg^{-1} soil and transferred into large PVC pots (Ø 19.1 cm and height 25 cm). These applications were used as representative for rather low, intermediate, and high EOM doses commonly applied in agricultural practices under field conditions, and they correspond to 1.75, 5.25, and 17.5 Mg ha^{-1} assuming a depth of 25 cm and a bulk density of 1.4 g cm^{-3}. Unamended controls were also included for both soil textures. Based on pre-tests, soil bulk densities of 1.35 and 1.25 g cm^{-3} were employed for the sandy loam and silt loam soils, respectively, as soil structural integrity was sufficiently intact at these densities, while minimal soil compaction was required for core filling. The sandy loam and silt loam soils were amended with 34 and 20 mg NO_3^--N kg^{-1}, respectively, by mixing a KNO_3 solution to adjust the soil N concentration to 35.7 mg NO_3^--N kg^{-1} (equivalent to 150 kg N ha^{-1} as per surface area assuming a depth of 30 cm and a bulk density of 1.4 g cm^{-3}). By adding mineral N, we aimed to exclude the possibility of dosage effects by differences in soil mineral N availability. Soil moisture was maintained at 55% water-filled pore space by adding demineralized water to the top of the soil cores. The packed soil macrocosms were covered with perforated parafilm to enable gas exchange but limit evaporation and were stored in a dark room at a constant temperature of 20±1.0 °C. Soil moisture was kept constant throughout the incubation experiment by regularly weighing the soil pots and replenishing evaporation water loss with demineralized water. The experiment comprised two soil textures × (three EOM application doses + unamended controls) × three replicates, yielding 24 soil macrocosms.

2.3 Soil CO_2 efflux measurements, isotopic analysis and source partitioning of soil C mineralization

Soil CO_2 efflux rates were obtained 14 times during the 90-day experiment by measuring the CO_2 build-up over time in an opaque closed PVC chamber headspace (8.45 l) on top of each of the PVC tubes with the soil macrocosms. The closed chamber was outfitted with a battery-powered fan and a pressure vent. Changes in headspace CO_2 concentrations and their $\delta^{13}C$ (in ‰ relative to the international Vienna Pee Dee Belemnite standard) resulting from soil CO_2 emissions were measured in real time by consecutively connecting a cavity ring-down spectroscopy analyser (G2201-i CRDS isotopic CO_2/CH_4 analyser, Picarro, United States) to each headspace chamber. A linear increase in CO_2 was recorded every 1–2 s for ~10 min or less to avoid excessive build-up of headspace CO_2 which could cause a drop in the diffusion gradient within the soil in treatment/time combinations during high microbial respiration. A linear model was fitted to the observed increase in headspace CO_2 concentration, and the soil CO_2 efflux rate was obtained from its slope and converted into a mass-based unit (mg kg^{-1} day^{-1}) using the ideal gas law. $\delta^{13}C$ of the emitted CO_2 was determined as the intercept of the linear regression line between the headspace air $\delta^{13}C$ and reciprocal of the headspace CO_2 concentration (Keeling, 1958).

The efflux of CO_2 derived from ryegrass mineralization was calculated by the following isotopic mixing model (Mendoza et al., 2022a):

$$CO_2\text{-}C_{(ryegrass)} = CO_2\text{-}C * \frac{\delta^{13}C\text{-}CO_2 - \delta^{13}C\text{-}CO_{2(0)}}{\delta^{13}C\text{-}CO_{2(ryegrass)} - \delta^{13}C\text{-}CO_{2(0)}} \quad (1)$$

where $CO_2\text{-}C$ is the overall soil CO_2-C efflux rate, $\delta^{13}C\text{-}CO_2$ is the isotopic signature of the respired CO_2 estimated using the Keeling plot, $\delta^{13}C\text{-}CO_{2(ryegrass)}$ is the estimated isotopic signature of emitted CO_2 resulting from ryegrass mineralization (Eq. 2), and $\delta^{13}C\text{-}CO_{2(0)}$ is the isotopic signature of CO_2 measured from treatments with no ryegrass added (i.e. resulting from SOC mineralization only).

https://doi.org/10.5194/egusphere-2024-107
Preprint. Discussion started: 30 January 2024

Isotopic fractionation of CO_2 caused by either microbial mineralization or diffusive transport to the headspace air was estimated separately for SOC and ryegrass EOM. The isotopic signature of the SOC-derived CO_2 measured in the unamended treatments was used to estimate C isotopic fractionation during SOC mineralization and diffusive SOC-derived CO_2 transport to the headspace air. The isotopic fractionation of ryegrass-C mineralization and its diffusive transport to the headspace air was estimated as the shift in $\delta^{13}C$ of the CO_2 emitted from the highest EOM dose (i.e. from ryegrass + SOC) and CO_2 emissions from the unamended control (i.e. from SOC), following a mass balance analogous to Keeling (1958), as follows:

$$\delta^{13}C\text{-}CO_{2(ryegrass)} = \frac{CO_2\text{-}C_{(5)} * \delta^{13}C\text{-}CO_{2(5)} - CO_2\text{-}C_{(0)} * \delta^{13}C\text{-}CO_{2(0)}}{CO_2\text{-}C_{(5)} - CO_2\text{-}C_{(0)}} \quad (2)$$

where $CO_2\text{-}C_{(5)}$ and $CO_2\text{-}C_{(0)}$ are the total CO_2-C fluxes corresponding to ryegrass doses of 5 and 0 g kg^{-1} soil measured at each soil texture, and $\delta^{13}C\text{-}CO_{2(5)}$ and $\delta^{13}C\text{-}CO_{2(0)}$ are the respective $\delta^{13}C\text{-}CO_2$.

The CO_2-C derived from SOC mineralization in the amended soils, $CO_2\text{-}C_{(SOC)}$ (mg CO_2-C kg soil day^{-1}), was calculated as follows:

$$CO_2\text{-}C_{(SOC)} = CO_2\text{-}C - CO_2\text{-}C_{(ryegrass)} \quad (3)$$

Finally, the cumulative amounts of mineralized ryegrass C and SOC were calculated. The priming effect (PE) of SOC mineralization induced by EOM application dose was calculated for each soil texture as follows:

$$PE_{(SOC)} = CO_2\text{-}C_{(SOC)} - CO_2\text{-}C_{(0)} \quad (4)$$

2.4 Microbial biomass carbon and soil mineral nitrogen

Eight additional soil macrocosms (four EOM doses: 0, 0.5, 1.5, and 5 g kg^{-1} soil × two soil textures: sandy loam and silt loam) were prepared as described in Section 2.2, but employing non-labelled ryegrass grown under the same environmental and edaphic conditions as the ^{13}C-labelled grass. After 45 days, soil was sampled, and microbial biomass carbon (MBC) was quantified using the fumigation-extraction method (Vance et al., 1987). Before and after fumigating fresh soil samples with ethanol-free chloroform, 30 g of soil was extracted with 60 ml 0.5 M K_2SO_4. These extracts were passed through a filter (Whatman 5) and analysed for their dissolved OC concentration using a TOC analyser (TOC/TN analyser, Skalar, The Netherlands). MBC was determined as the difference in extractable C between fumigated and non-fumigated soils, and corrected with a factor of 0.45 to account for the MBC fraction extractable by fumigation (Joergensen, 1996). The EOM-mediated MBC increase was also calculated for each application dose to test whether MBC was proportionally stimulated per unit of EOM added.

At the end of the 90-day incubation experiment, soil from each macrocosm was destructively sampled and mineral N was determined. The soil was taken out of the PVC pots, homogenised, from which 20 g was weighed and shaken with 100 ml 1 M KCl for one hour, and the extracts were filtered (Macherey-Nagel, USA, MN 616 1/4, Ø 150 mm filters). NH_4^+-N and NO_3^--N concentrations in the extracts were measured using a continuous-flow analyser (Skalar, San++ Continuous Flow Analyser, Netherlands). Soil NH_4^+-N was negligible in all treatments; therefore, only NO_3^--N concentrations were considered.

2.5 Soil redox potential

The soil redox potential (Eh) was measured 21 times during the 90-day incubation experiment in each of the 24 macrocosms. Every soil core was permanently outfitted with one Ag|AgCl saturated KCl reference electrode and a redox probe (Paleoterra, Netherlands). The redox probes consisted of two platinum sensors (surface area ±5 mm^2 each) situated

https://doi.org/10.5194/egusphere-2024-107
Preprint. Discussion started: 30 January 2024

5 cm and 15 cm below the soil surface. The reference electrodes and redox probes were first tested and calibrated with 124 and 250 mV redox standards (Sigma-Aldrich, Ireland). Soil Eh readings were obtained by connecting the reference and Pt electrodes through a high-impedance redox mV meter (Paleoterra, The Netherlands). The Eh readings were expressed versus the standard hydrogen electrode after temperature and offset corrections with the Ag|AgCl reference electrode by adding 204 mV to the mV readings.

2.6 Pore neck size distribution

Four intact soil cores were carefully sampled using stainless-steel sampling rings (Ø 5.0 cm and height 5.1 cm) from each of the eight macrocosms described in Section 2.4. These rings were used to determine the soil water retention curve using the sandbox pressure plate method. After fitting a nylon mesh onto the bottom of the rings, they were placed on a sand box apparatus (Eijkelkamp Agrisearch Equipment, Giesbeek, Netherlands), saturated, subjected to pressure potentials of -10, -30, -50, -70, and -100 hPa, and weighed for the corresponding soil water content after reaching equilibrium. The soil water content at soil matric potentials of -330, -1000 and -15000 hPa were determined using pressure plates (Eijkelkamp Agrisearch Equipment, Giesbeek, Netherlands and Soil Moisture Equipment, Santa Barbara, CA, USA). Volume of the soil pore neck size classes corresponding to these water potentials was calculated using Jurin's law: $d = -3000/\Psi$, where d is the pore neck diameter (µm) and Ψ the matric potential (hPa) (Schjønning et al., 1999). Consequently, the volume proportion (vol%) of pores with pore neck diameters of >300, 100–300, 60–100, 43–60, 30–43, 9–30, 3–9, 0.2–3, and <0.2 µm were calculated.

2.7 Statistical analyses

General linear models (GLM) were used to evaluate the effects of EOM dose and soil texture on EOM and SOC mineralization, MBC, EOM-mediated MBC increase, and soil mineral N. Exponential functions explaining the mineralized proportion of EOM and the EOM-mediated MBC increase were assessed by log transformation of these variables prior to the GLM. If the GLM showed a significant interaction between EOM dose and soil texture, separate GLMs with different EOM doses were conducted per soil texture. In the case of no interaction, the interaction term was removed from the model and an additive model was built with the EOM dose and soil texture. Additionally, one-way analysis of variance (ANOVA) was conducted for each soil texture to check the effects of EOM dose on the vol% of pore neck size classes and soil Eh at each measurement time. Linear mixed models (LMM) were used to compare the effects of EOM dose on soil Eh with the fixed effects of EOM dose, measurement depth, interaction depth × dose, and random effects of time and replicate. Normality was assessed by the QQ plots of the residuals, and homoscedasticity was verified by plotting residuals versus fitted values. The Shapiro-Wilk's test and Levene's test were used to confirm the normality of the distributed model residuals and equality of variances, respectively. Pearson's correlation coefficients were calculated for the selected variables. All statistical tests were conducted with R version 3.6.1, using the packages car and agricolae for GLM and one-way ANOVA, lme4 for LMM, and hmisc and ggpubr to detect correlations between the variables.

3 Results

3.1 EOM mineralization

The amount of mineralized EOM increased linearly after 90 days with the EOM application dose for both textures (P <0.001), with determination coefficients close to 1. Less EOM was mineralized in the sandy loam than in the silt loam soil, with values of 223 and 279 mg C per added gram of EOM, respectively (Figure 1 top). The relative fraction of added EOM mineralized after 90 days depended on the soil texture. In the sandy loam soil, it was independent of EOM

https://doi.org/10.5194/egusphere-2024-107
Preprint. Discussion started: 30 January 2024

application dose, whereas in the silt loam soil, the relative fraction of mineralized EOM decreased with increasing EOM dose (P <0.05; Figure 1 bottom).

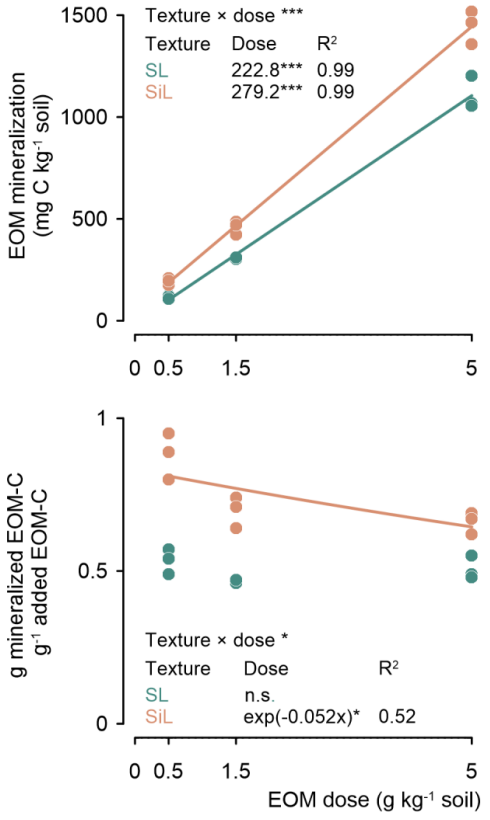

Figure 1. Cumulative mineralized EOM C (ryegrass) after 90 days since incorporation in sandy loam (SL) or silt loam (SiL) soil as a function of its application dose (upper figure). The lower figure presents the proportion of mineralized ryegrass C as a function of EOM dose. * denote significance levels of the linear model interaction effect between soil texture and EOM dose, and for the linear or exponential response of EOM mineralization to EOM dose, with *** <0.001, ** <0.01, * <0.05, and n.s. = not significant.

3.2 SOC mineralization

After 90 days of incubation, the cumulative mineralized SOC increased linearly with increasing application dose in both soils and this dosage response was stronger in the silt loam soil (117.2 mg C per g EOM) (P <0.001) compared with the sandy loam soil (49.6 mg C per g EOM) (Figure 2 top).

EOM application dose also stimulated native SOC mineralization. Such positive priming of SOC was stronger in the silt loam soil, where SOC mineralization increased by 124.6 mg C per g EOM added compared with the unamended control, than in the sandy loam soil, where the increase in SOC mineralization was 50.3 mg C per g EOM added (P <0.001; Figure 2 bottom).

https://doi.org/10.5194/egusphere-2024-107
Preprint. Discussion started: 30 January 2024

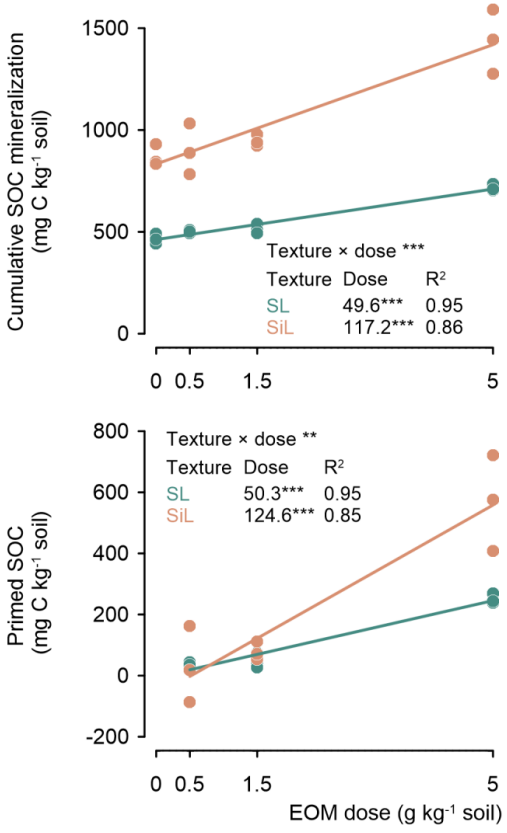

Figure 2. Cumulative mineralized native SOC (mg C kg^{-1}) after 90 days for a sandy loam (SL) and a silt loam (SiL) soil as a function of EOM (ryegrass) application dose (upper figure). The lower graph compares the extra amount of SOC mineralized vs. the unamended controls, i.e. EOM addition induced priming of native SOC in both soil textures. * denote significance levels of the linear model interaction effect between soil texture and EOM dose, and for the linear response of cumulative and primed SOC mineralization to EOM dose, with *** <0.001, ** <0.01, * <0.05, and n.s. = not significant.

3.3 Soil microbial biomass

MBC was linearly related to the EOM dose after 45 days of incubation (P <0.001; Figure 3 top). The increase in MBC in response to increasing EOM dose was double in the silt loam compared with the sandy loam soil, i.e. +25.3 and +12.3 mg MBC per gram EOM added, respectively. The resulting overall increase in MBC was not proportional to the EOM dose; therefore, EOM-mediated MBC increase (i.e. the extra MBC in the EOM-amended vs. control soil) to the EOM dose tended to decrease with EOM dose, although not significantly (P = 0.428; R^2 = 0.15; Figure 3 bottom).

https://doi.org/10.5194/egusphere-2024-107
Preprint. Discussion started: 30 January 2024

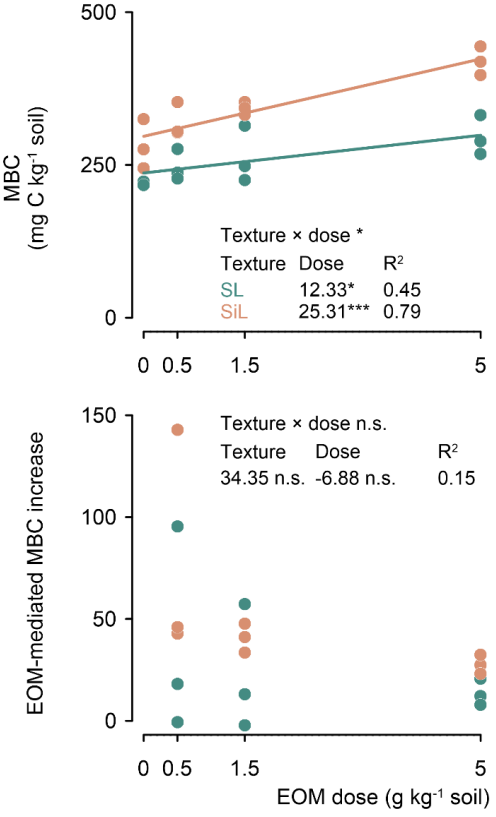

Figure 3. Microbial biomass carbon (MBC) after 45 days of incubation of the sandy loam (SL) and silt loam (SiL) soils amended with EOM (ryegrass) at various application doses (upper figure). The corresponding EOM-mediated MBC increase is presented in the lower figure. * denote significance levels effects of the linear model interaction between soil texture and EOM dose, and the effect of EOM dose on MBC and EOM-mediated MBC increase, with *** <0.001, ** <0.01, * <0.05, and n.s. = not significant.

3.4 Soil redox potential

Soil Eh varied from approximately +550 to +850 mV in the sandy loam soil cores (Figure 4). It tended to decrease with increasing EOM dose until five days from the start of the incubation, after which it became indifferent with EOM addition; although in the control treatment, it mostly remained above the Eh in the EOM-amended soils. Nevertheless, no significant differences were observed in Eh between the EOM treatments in the sandy loam soil. In the silt loam soil, overall Eh was lower than that in the sandy loam soil and varied from approximately +470 to +700 mV. Although Eh in the silt loam soil was consistently lower for the 5 g kg^{-1} soil EOM treatment during the first 41 days, the dose effect was not statistically significant, despite six replicate measurements per treatment. Overall, for both soils, the observed Eh ranges indicated prevailing oxic conditions (>300 mV), with O_2 being the main electron acceptor used in microbial respiration (Reddy and DeLaune, 2008). The non-significant interaction between dose × depth (5 and 15 cm below surface) for both soil textures demonstrated that the dosage effect on soil Eh did not differ among soil depths.

https://doi.org/10.5194/egusphere-2024-107
Preprint. Discussion started: 30 January 2024

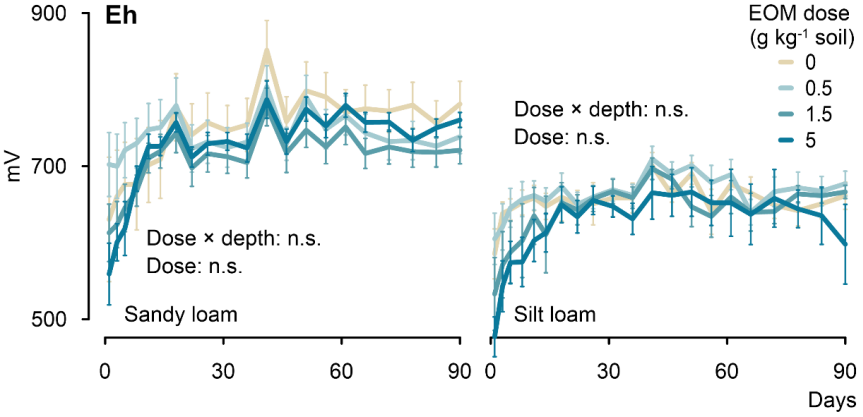

Figure 4. Evolution of the soil redox potential measured at 5 and 15 cm depth across the 90-day incubation experiment for the sandy loam and silt loam soils amended with different doses of EOM (ryegrass). Error bars show standard errors of means (n = 6).

3.5 Soil pore structure

In sandy loam soil, no effect of EOM addition was observed on the pore neck size distribution (Figure 5). However, in case of the 5 g kg^{-1} soil EOM dose, a reduction of the 3–9 µm class vol% by 20% compared with the unamended control (P <0.05) was observed. In silt loam soil, EOM application more strongly affected the pore neck size distribution, especially at higher EOM doses. Adding EOM at 1.5 and 5 g kg^{-1} soil increased the vol% of the >300 µm pore class by 48% and 49%, respectively, compared with the control (although only at P <0.1). Addition of 5 g EOM kg^{-1} also increased the volume fraction of the 60–100 µm class by 21% compared with the control (P <0.05). The 43–60 µm class volume fraction was also larger in the 5 g kg^{-1} soil EOM treatment than in the 0.5 g kg^{-1} soil treatment (P <0.05). EOM doses of 0.5, 1.5, and 5 g kg^{-1} soil increased the volume fraction of the 3–9 µm class by 50%, 62%, and 32%, respectively (P <0.05). In contrast, there was a decrease in the volume fraction of the 0.2–3 µm pore size class by 12%, 20%, and 17% with EOM doses of 0.5, 1.5, and 5 g kg^{-1}, respectively (P <0.01).

https://doi.org/10.5194/egusphere-2024-107
Preprint. Discussion started: 30 January 2024

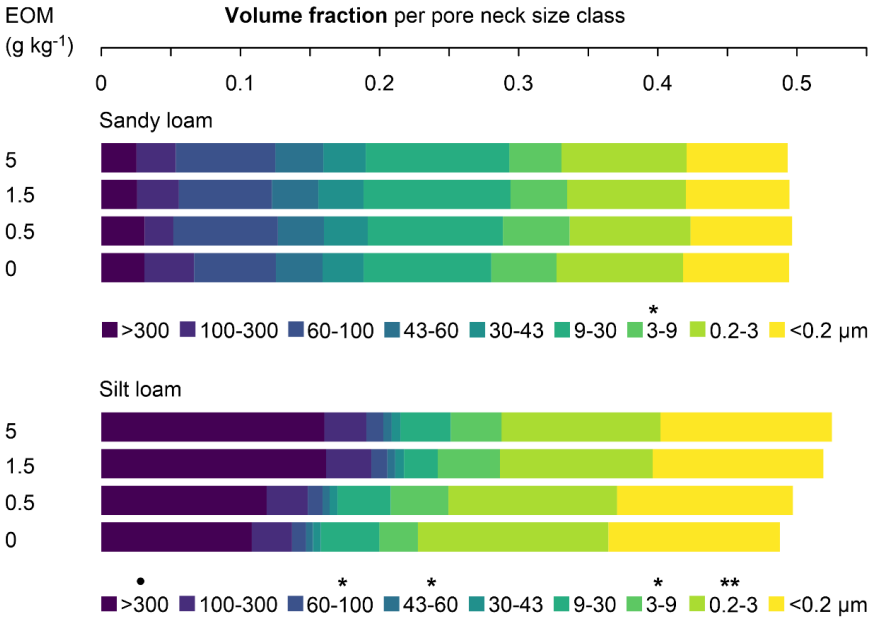

Figure 5. Volume fraction (unitless) of nine pore neck size classes (i.e. pores with given intervals of the pore neck diameter) in the sandy loam and silt loam soils after the application of EOM (ryegrass) doses and an unamended control (n = 4). * represent significant differences (one-way ANOVA) of the volume fraction of the pore neck class between EOM doses within each soil texture, with *** < 0.001, ** <0.01, * <0.05, and • <0.1.

3.6 Soil mineral nitrogen

Soil mineral N measured after 90 days of incubation increased linearly with EOM dose in both sandy loam and silt loam soils (P <0.001; Figure 6). It was always higher in the EOM-amended treatments than in the unamended controls. In the sandy loam soil, soil mineral N increased more strongly with EOM dose than in the silt loam soil, with values of +13.1 vs. +6.9 mg N per g EOM added, respectively.

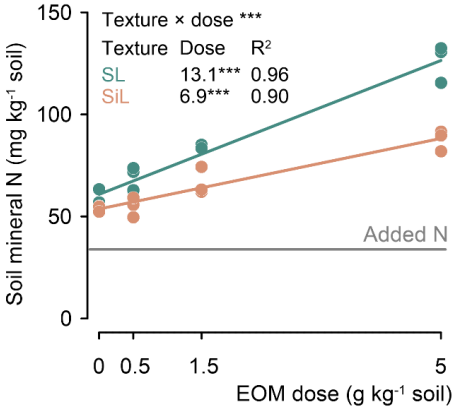

https://doi.org/10.5194/egusphere-2024-107
Preprint. Discussion started: 30 January 2024

Figure 6. Soil mineral nitrogen (NO_3^--N) content at the end of the 90-day incubation as a function of EOM dose for a sandy loam (SL) and a silt loam (SiL) soil. * denote significance levels of the linear model variables soil texture and EOM dose and their interaction on soil mineral N, with *** <0.001.

4 Discussion

4.1 Mineralization of EOM as a function of its application dose

In the sandy loam soil, EOM-derived C mineralization was independent of its application dose, whereas it decreased exponentially with increasing EOM dose in the silt loam soil (Figure 1), contradicting our hypothesis that the relative EOM mineralization would increase with increasing EOM dose. Overall, around 50 and 75% EOM-C was mineralized in the sandy loam and silt loam soils after the 90-day incubation experiment (Fig. 1). The ordination of relative EOM mineralization patterns remained consistent among the established dose treatments over time and are projected to remain likewise for at least some time (Fig. A1). For instance, mineralization over 137 days at the established 20°C in the lab experiment equates to about one year in the field in Belgium (9.7°C on average) (De Neve et al., 1996). Thus, the present analysis suggests that within the time scale of about one year we might expect no dosage response of EOM mineralization in the sandy loam soil and a negative response with dose for the silt loam soil. The unresponsiveness of relative EOM mineralization to EOM application dose in the sandy loam soil was consistent with the results of (Shahbaz et al., 2017a), who observed equal relative degradation of wheat crop residue with EOM dose of 1.40 and 5.04 g kg^{-1}. We previously also found the response of maize straw C mineralization to be unresponsive to its application dose in soils with contrasting native soil organic matter (SOM) levels (Mendoza et al., 2022a), and likewise for ryegrass (Mendoza et al., 2022b). These results are, however, in contrast to a study by Don et al. (2013), who reported that the mineralization of total soil C (SOC and EOM) was much slower when compost was diluted in a soil column than when it was concentrated. They postulated that higher proximity between the substrate and decomposers would allow more efficient decomposition. In contrast, here, the EOM-mediated MBC increase tended to decrease with increasing EOM dose (Fig. 3; bottom), suggesting that further growth of MBC was energetically less favourable with increasing substrate concentrations. This is in line with Ekschimitt et al. (2005), who postulated, based on the modelling output of an inverse Michaelis-Menten equation, that as the enzyme pool increases, the activity per unit enzyme decreases, with a lower relative C decomposition at higher C concentrations. They concluded that energy costs are not returned by decomposition products over a certain enzyme production rate, creating a negative feedback loop for microbial activity. Although similar explanations may exist for the unresponsiveness of EOM mineralization to dose in the sandy loam soil, other mechanisms should be considered to explain the even surprising negative impact of EOM dose on its mineralization in silt loam soil.

Various factors could have increasingly restricted soil heterotrophic activity with increasing EOM dose in the silt loam soil. First, with an abundance of labile C added, as was the case here, a shortage of mineral N could have limited microbial growth. However, such an effect could be excluded because high soil N concentrations (>50 mg NO_3^--N kg^{-1}) were observed at the end of the experiment in all treatments, likely as a result of the initial large added dose of N (35.7 mg NO_3^--N kg^{-1}) and net N mineralization from EOM, indicated by the proportional increase of final mineral N content to EOM dose (Fig. 6). Second, the increase in MBC and microbial respiration caused by high EOM doses could result in excessive O_2 demand that, when not met by O_2 diffusion could limit EOM degradation. Such O_2 limitations due to higher EOM doses may be expected to be more severe in finer-textured soil due to lower air permeability. Soil Eh was indeed generally lower in the silt loam soil than in the sandy loam soil, and increasing EOM dose more strongly decreased the soil Eh in silt loam soil, but still Eh remained at levels indicative of aerobic conditions (Fiedler et al., 2007; Husson, 2013). Furthermore, as NO_3^- concentrations increased with increasing EOM dose, there was no indication of more denitrification with increasing EOM dose. The overall oxidised soil state, even in the finer-textured soil with a high dose

https://doi.org/10.5194/egusphere-2024-107
Preprint. Discussion started: 30 January 2024

of EOM, might be linked to the development of the soil pore network, namely, high EOM doses significantly increased the vol% of larger pore neck classes (i.e. 43–60, 60–100, and >300 µm) in the silt loam soil. Hence, from the Eh readings, we observed no indication that O_2 limitations would have caused the lower relative EOM mineralization in the silt loam soil at higher EOM doses. In conclusion, we could not identify the cause of these phenomenon, and further research is required to explore the potential mechanisms leading to a relative temporal stabilization of EOM when added at larger doses. For example, occlusion of EOM in soil aggregates is known to provide some degree of physical protection against decomposition, but the effect of EOM dose thereupon was not assessed in this study. Soil aggregate formation is stimulated by OM addition, and De Gryze et al. (2005) reported greater development of macroaggregates at higher EOM doses. Therefore, it would be reasonable to postulate and further investigate that physical protection of EOM by aggregate occlusion is favoured at higher application doses, causing negative feedback on the relative EOM mineralization.

Drawing conclusions for EOM management in the field based on this 90-day lab incubation experiment at 20°C is to be made with care. Nevertheless, well aligned temporal courses of the cumulative EOM mineralization (Fig. A1) suggest at least on the short term an unchanged ordination of further relative EOM mineralization between the dose treatments. When extrapolated to 137 days (not shown), more or less equivalent to C mineralization occurring in one year in the field at 9.7°C in Flanders (De Neve et al., 1996), our results suggest no or but a limited negative effect of adding EOM at increasing doses on its annual mineralization, a traditionally used metric in C-balance calculations (the so-termed humification coefficient). However, empirical evidence from field experiments is now needed to confirm these findings.

4.2 Effect of EOM application dose on native SOC mineralization

We hypothesized that SOC mineralization would be stimulated by increasing the EOM dose with stronger effects in sandy loam soil, as SOC may be less stabilized than in silt loam soil. Priming of SOC mineralization was linearly related to the ryegrass application dose (P <0.001), with native SOC mineralization stimulated by 50 and 125 mg C per gram of EOM added in the sandy loam and silt loam soils, respectively (P <0.001). Shahbaz et al. (2017a) reported that addition of ground wheat residue of 1.40 and 5.04 g kg^{-1} soil to a silt loam soil increased SOC mineralization by 50% and 90%, respectively. In our study, SOC mineralization increased by 8%, 10%, and 54% in the sandy loam soil, and by 4%, 9%, and 65% in the silt loam soil from the low to high EOM doses. In agreement with our study, a positive linear relationship between glucose dose (0.008 to 1.606 g C kg^{-1} $week^{-1}$) and SOC priming was reported by Liu et al. (2017). In contrast, Xiao et al. (2015) reported a decrease in the priming of SOC per unit of litter (mix of <2 mm aboveground plants of a steppe vegetation) added (0, 60, 120, 240, and 480 g C m^{-2}). Moreover, Guenet et al. (2010) reported that addition of wheat straw (3.5, 5.2 and 7.5 g kg^{-1} soil) did not stimulate proportional SOC mineralization. These outcomes are in contrast with the observed proportional priming of SOC with increasing EOM in this study. Nitrogen availability did not likely limit heterotrophic activity in our study, but it possibly did restrict C mineralization at increasing EOM doses in the experiments of Guenet et al. (2010) and Xiao et al. (2015). A commonly proposed mechanism to explain SOC priming is the 'N-mining theory' (Craine et al., 2007), which assumes that microbes decompose native SOC in search of mineral N to meet their metabolic demands. As explained above, with extra mineral N added initially to our soils and a clear further net soil N mineralization, this mechanism can largely be ruled out. Alternatively, SOC priming is often explained by the 'co-metabolism hypothesis (Bingeman et al., 1953; Kuzyakov and Domanski, 2000), i.e. application of a labile substrate, such as the ryegrass used here, stimulates microbial biomass growth and enzyme production, which in addition to decomposing EOM, also triggers native SOC mineralization. MBC was linearly related to the EOM dose in both soils (Figure 3) and positively correlated with the rate of SOC priming in both sandy loam and silt loam soils (r = 0.63 and 0.72, respectively; P <0.05). While these trends support the idea that increased microbial biomass and activity with EOM addition primed SOC mineralization, further proof is required to identify co-metabolism as the principal mode of SOC

https://doi.org/10.5194/egusphere-2024-107
Preprint. Discussion started: 30 January 2024

priming. Most studies (e.g. Xiao et al. (2015)) have shown that priming of SOM mineralization relates linearly to MBC but indeed likewise could not unequivocally pinpoint the mechanisms involved. An overall stronger priming of SOC in the silt loam soil, regardless of EOM dose, likely results from an inherent better SOC degradability compared to the sandy loam soil, as evidenced by the much higher MBC and SOC mineralization in the unamended control soils (Fig. 2 and Fig. 3). This contrast in MBC and heterotrophic activity is unlikely to have been the result of differences in SOC content, content of pedogenic oxides or pH, as these properties were very similar between both textured soils. Instead, this more likely results from a combination of differences in SOC quality and soil physical structure between both textures, but such effects are difficult to discriminate from one another.

The duration of the present 90-day incubation experiment was sufficiently long to capture trends in SOC priming. The temporal course of the SOC priming response to EOM dose was also similar in both textured soils. In sandy loam soil, increasing EOM dose induced higher positive SOC priming between days 2 and 12 of the incubation (1.5 g kg^{-1} soil vs. control, $P = 0.03$; 5 g kg^{-1} soil vs. control, $P < 0.001$), whereas priming was not significant from day 12 on. In silt loam soil, SOC priming occurred between days 2 and 17 of the incubation (5 g kg^{-1} soil vs. control, $P = 0.001$) but no longer thereafter (Fig. B1). As SOC priming was thus rather short-lived, this allows careful projections for the relevance of EOM dose responses on priming in the overall SOC balance. After comparing the EOM and SOC priming responses to EOM doses, intermediate applications of 1.5 and 5 g kg^{-1} soil would seem to reduce the overall C mineralization (i.e. from EOC and SOC priming) by 20% and 10% compared to 10 split doses of 0.5 g kg^{-1} soil. Thus, splitting EOM applications into small doses would adversely impact SOC stocks, while splitting into intermediate doses, i.e. 1.5 g kg^{-1} soil, which is close to current common agricultural practice, might be a better option to maintain SOC stocks. However, these suggestions should be managed with great care since in this experiment we did not test the effect of repeated EOM doses. Finally, it is important to note that formation of new SOC from decomposing EOM was not considered here, although this would yield a more accurate prediction of the net effect of EOM doses on the SOC balance. Our experimental set-up did not allow the detection of remnant EOM and newly formed SOC against the native SOC background. Although not confirmed statistically, it is noteworthy that, especially for silt loam soil, less MBC was produced per unit of EOM added. Microbial biomass-derived necromass contributes to SOC formation (Kästner et al., 2021) and according to Liang et al. (2019) can make up to 56% of the total SOC in temperate agricultural soils. A relative decrease in the formed MBC per unit of EOM added might thus adversely impact SOC preservation when EOM is added at fewer but larger doses. Ultimately, long-term field observations are again required to confirm the impact of EOM dosage on SOC storage.

4.3 Effect of soil pore structure on priming of SOC mineralization

We also investigated whether EOM application dose affected soil structure and if this in turn explained the priming of SOC mineralization. We did not observe major changes in the soil structure with respect to different EOM doses in the sandy loam soil. However, EOM stimulated the volume percentage of several larger pore classes (43–60, 60–100 and >300 µm; $P < 0.05$, 0.05, and 0.1, respectively) in the silt loam soil. This development of macroporosity might have promoted priming of SOC in the silt loam soil. In fact, there were positive linear relationships (via linear regressions) between the silt loam soil volume fraction of pore neck size classes 60–100 and >300 µm and SOC priming ($R^2 = 0.34$ and 0.36; and, $P = 0.09$ and 0.08, respectively), and a negative relation with the 3-9 µm class that also depended on EOM dose, whereas no such relationships existed for the sandy loam soil. The contrasting unresponsiveness of EOM mineralization to EOM dose as compared to SOC priming could be explained as follows. In particular, the majority of SOC is usually mineral-associated in agricultural soils (Kögel-Knabner et al., 2008), and is therefore situated within small pores where oxygen provision can be readily constrained (Kuka et al., 2007), while the added discrete substrate particles necessarily reside in large macropores, due to which SOC and not EOM mineralization may sooner become O_2 limited.

https://doi.org/10.5194/egusphere-2024-107
Preprint. Discussion started: 30 January 2024

Mineralization of SOC would therefore be logically more dependent on moderation of soil structure towards more macropores caused by EOM amendment. Experimental verification of this hypothesis will be challenging as spatial mapping of O_2 availability in soil pore space is practically difficult. We further compared the results with our previous study using the same soils (although sampled at different times in the field) and exactly the same source of EOM (although more refined) as used here. In the previous study, ryegrass doses of 0.5 and 5 g kg^{-1} soil stimulated macroporosity formation and SOC mineralization by 30% and 71% in sandy loam soil, but only by 28% in silt loam soil at high dose when the soil structure was apparently unaffected (Mendoza et al., 2022b). Due to differences in initial soil disturbance, in the current experiment, the silt loam soil had a much larger fraction of very small pores (>10% of the soil volume consisted of <0.2 µm pores) when compared to that in (Mendoza et al., 2022b). Improved soil aeration, which likely resulted from the increase in the vol% of >300, 60–100, and 43–60 µm pore classes with EOM added, could thus again explain the stronger observed stimulation of SOC mineralization in this study, when compared to (Mendoza et al., 2022b). The soil Eh data did not indicate improved aeration in the silt loam soil at higher EOM application doses, but this was not necessarily expected because the two phenomena that co-determine Eh probably counterbalanced each other as follows: improved aeration and a corresponding increase in Eh with more EOM added vs. more heterotrophic activity (and corresponding electron donation). In conclusion, we postulate that macroporosity induced by OM application could indirectly stimulate native SOC mineralization, particularly when a large part of the pore space is composed of very small pores. An overview of the main mechanisms by which EOM application dose affects the relative EOM and native SOC mineralization is presented in Figure 7.

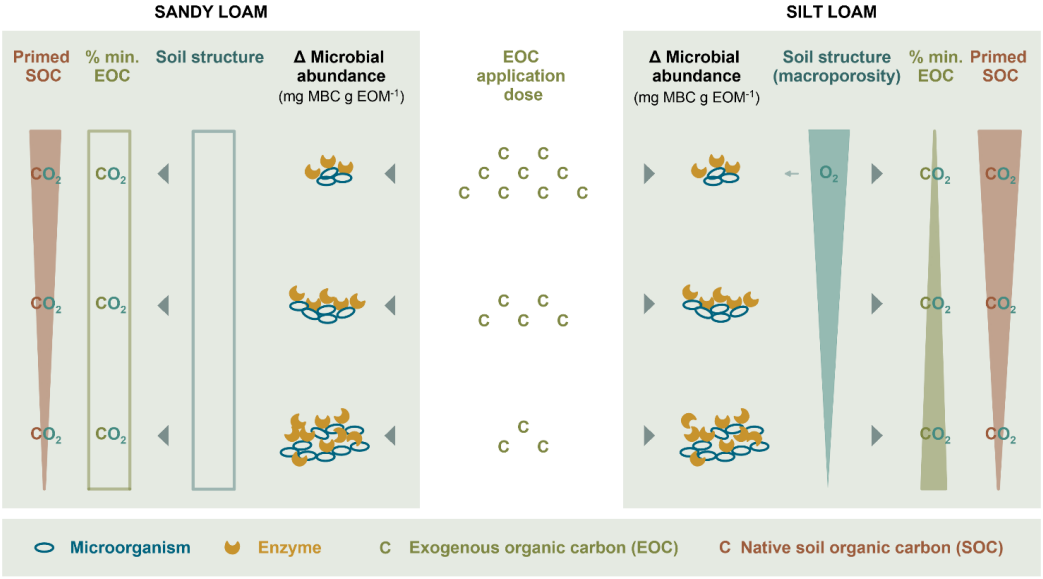

Figure 7. Overview of the mechanisms shaping the relative EOC mineralization (% min. EOC) and SOC priming effects in response to EOM application dose. In the sandy loam soil (left-hand side), increasing EOM dose supplied energy for microbial growth and extracellular enzyme production, which possibly degraded native SOC (i.e. co-metabolism), but did not affect the mineralized EOM fraction. Soil Eh decreased slightly with increasing EOM dose, but C mineralization remained aerobic as expected in the sandy loam soil. Here, soil structure was not much affected by EOM dose. In the silt loam soil (right-hand side), where O_2 diffusion is expected to

https://doi.org/10.5194/egusphere-2024-107
Preprint. Discussion started: 30 January 2024

be inherently constrained, increasing EOM dose induced macroporosity which also compensated the large O_2 consumption due to larger microbial growth. Here, not only co-metabolism but also soil structure could explain the positive priming effects with increasing EOM dose in the silt loam soil. The decreasing percentage of decomposed EOM with increasing EOM application dose observed in the silt loam soil could be better explained by the EOM-mediated increase in MBC, which tended to decrease with higher application dose.

5 Conclusion

Limited research exists on the effect of EOM dose on C mineralization in soil, and consequently, this effect has also been largely overlooked by SOC simulation models. Our results showed a dose response of EOM mineralization in heavy- but not light-textured soil, and priming of native SOC that was proportional to the EOM dose in both soils. Interestingly, the stimulation of SOC mineralization in silt loam soil correlated with stronger development of macroporosity. Such soil structure formation caused by OM addition may be a relevant yet largely unconsidered avenue through which SOC priming occurs. Revealing causality with experiments targeting changes in soil structure with perhaps local O_2 measurements at the microscale where SOC resides could be the way forward to gain mechanistical understanding of SOC priming from a physical view. Moreover, the observed negative response of relative EOM mineralization to a high dose remained elusive, and we suggest experimental verification of a possibly higher physical protection of the added EOM inside an aggregate-occluded fraction. Moreover, as we observed indications that in silt loam soil less MBC was produced per unit of EOM added, empirical evidence of the EOM dose contribution to SOC formation would be required. Finally, the findings of this upscale experiment should be confirmed in field conditions where environmental conditions vary as well as soil structure.

Appendix A

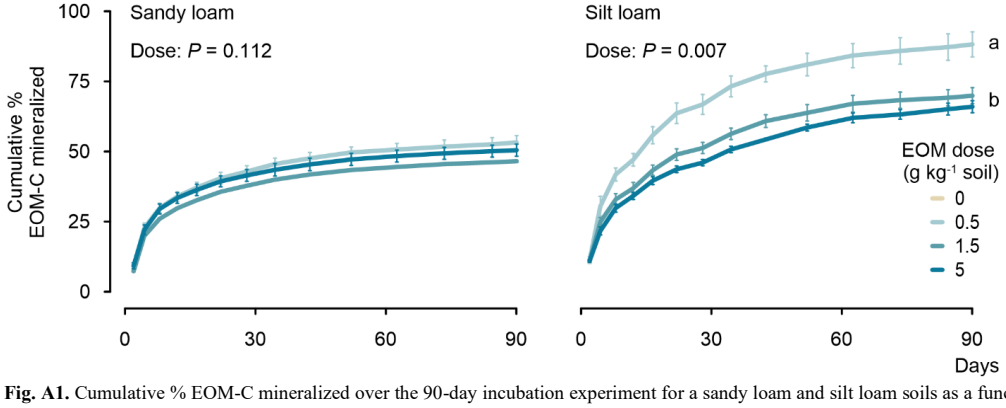

Fig. A1. Cumulative % EOM-C mineralized over the 90-day incubation experiment for a sandy loam and silt loam soils as a function of application dose. *P* values indicate the effect of application dose on the percentage of EOM mineralized at the end of the experiment. Error bars show standard errors of means (n = 3).

https://doi.org/10.5194/egusphere-2024-107
Preprint. Discussion started: 30 January 2024

Appendix B

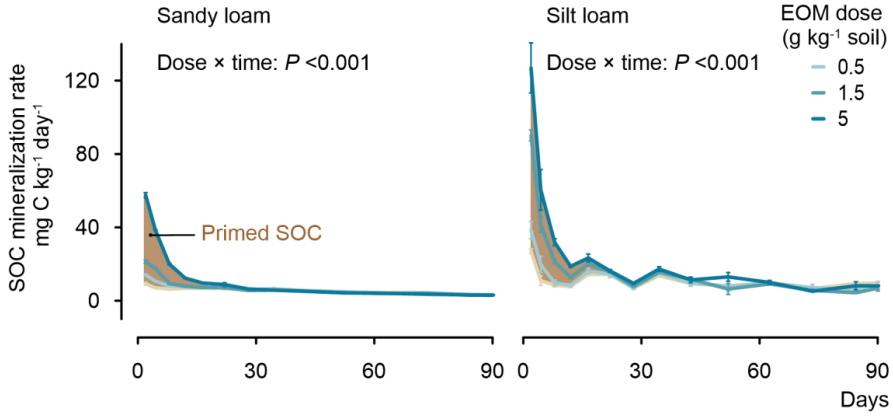

Fig. B1. The SOC mineralization rates over the 90-day incubation experiment for a sandy loam and a silt loam soil in response to EOM application dose. Shadow brownish areas depict priming of SOC mineralization caused by EOM application dose. In sandy loam soil, EOM dose induced SOC priming between days 2 and 12 of the incubation (*P* values for 1.5 g kg^{-1} vs. control = 0.03; 5 g kg^{-1} vs. control <0.001; 5 vs. 0.5 g kg^{-1} <0.001; and, 5 vs 1.5 g kg^{-1} <0.001), whereas priming remained not significant during day 12 to 90. In silt loam soil, EOM dose induced SOC priming between days 2 and 17 of the incubation (*P* values for 5 g kg^{-1} vs. control = 0.001; 5 vs. 0.5 g kg^{-1} = 0.002; and, 5 vs. 1.5 g kg^{-1} = 0.01), while priming was not significantly different between EOM doses from day 17 to 90. Error bars show standard errors of means (n = 3).

Data availability. The data generated in this study are available from the corresponding author upon reasonable request.

Author contributions. OM, SDN and SS conceptualized the study and acquired funding. OM, HD, HL, and AF performed the experiment. OM wrote the original draft, and all the authors edited and reviewed the manuscript.

Conflicts of interests. At least one of the (co-)authors is a member of the editorial board of SOIL.

Acknowledgments. This work was supported by the Research Foundation Flanders (FWO: G066020N). We acknowledge the Secretaría Nacional de Educación Superior, Ciencia, Tecnología e Innovación (Senescyt-Ecuador) for funding Orly Mendoza. We also thank Mathieu Schatteman, Tina Coddens, Anne-Mie Terryn, Sophie Schepens, Maarten Volckaert, and Thu Tran for their assistance during chemical and physical analyses and for setting up the experiments.

References

Bingeman, C. W., Varner, J., and Martin, W.: The effect of the addition of organic materials on the decomposition of an organic soil, Soil Sci. Soc. Am. J., 17, 34–38, 1953.

Blagodatskaya, E. V., Blagodatsky, S. A., Anderson, T. H., and Kuzyakov, Y.: Priming effects in Chernozem induced by glucose and N in relation to microbial growth strategies, Appl. Soil Ecol., 37, 95–105, https://doi.org/10.1016/j.apsoil.2007.05.002, 2007.

Craine, J. M., Morrow, C., and Fierer, N.: Microbial nitrogen limitation increases decomposition, Ecology, 88, 2105–2113, https://doi.org/10.1890/06-1847.1, 2007.

De Gryze, S., Six, J., Brits, C., and Merckx, R.: A quantification of short-term macroaggregate dynamics: influences of wheat residue input and texture, Soil Biol. Biochem., 37, 55–66, https://doi.org/10.1016/j.soilbio.2004.07.024, 2005.

De Neve, S., Pannier, J., and Hofman, G.: Temperature effects on C-and N-mineralization from vegetable crop residues, Plant Soil, 181, 25–30, 1996.

Don, A., Rödenbeck, C., and Gleixner, G.: Unexpected control of soil carbon turnover by soil carbon concentration, Environ. Chem. Lett., 11, 407–413, https://doi.org/10.1007/s10311-013-0433-3, 2013.

https://doi.org/10.5194/egusphere-2024-107
Preprint. Discussion started: 30 January 2024

Dungait, J. A., Hopkins, D. W., Gregory, A. S., and Whitmore, A. P.: Soil organic matter turnover is governed by accessibility not recalcitrance, Glob. Change Biol., 18, 1781–1796, https://doi.org/10.1111/j.1365-2486.2012.02665.x, 2012.

Ekschmitt, K., Liu, M., Vetter, S., Fox, O., and Wolters, V.: Strategies used by soil biota to overcome soil organic matter stability — why is dead organic matter left over in the soil?, Geoderma, 128, 167–176, https://doi.org/10.1016/j.geoderma.2004.12.024, 2005.

Fiedler, S., Vepraskas, M. J., and Richardson, J. L.: Soil Redox Potential: Importance, Field Measurements, and Observations, in: Advances in Agronomy, vol. 94, Elsevier, 1–54, https://doi.org/10.1016/S0065-2113(06)94001-2, 2007.

Garnier, P., Cambier, C., Bousso, M., Masse, D., Chenu, C., and Recous, S.: Modeling the influence of soil-plant residue contact on carbon mineralization: Comparison of a compartmental approach and a 3D spatial approach, Soil Biol. Biochem., 40, 2754–2761, https://doi.org/10.1016/j.soilbio.2008.07.032, 2008.

Guenet, B., Neill, C., Bardoux, G., and Abbadie, L.: Is there a linear relationship between priming effect intensity and the amount of organic matter input?, Appl. Soil Ecol., 46, 436–442, https://doi.org/10.1016/j.apsoil.2010.09.006, 2010.

Hénin, S. and Dupuis, M.: Essai de bilan de la matière organique du sol, Dudod, 1945.

Husson, O.: Redox potential (Eh) and pH as drivers of soil/plant/microorganism systems: a transdisciplinary overview pointing to integrative opportunities for agronomy, Plant Soil, 362, 389–417, https://doi.org/10.1007/s11104-012-1429-7, 2013.

Jenkinson, D. S., Poulton, P. R., and Bryant, C.: The turnover of organic carbon in subsoils. Part 1. Natural and bomb radiocarbon in soil profiles from the Rothamsted long-term field experiments, Eur. J. Soil Sci., 59, 391–399, https://doi.org/10.1111/j.1365-2389.2008.01025.x, 2008.

Joergensen, R. G.: The fumigation-extraction method to estimate soil microbial biomass: Calibration of the kEC value, Soil Biol. Biochem., 28, 25–31, https://doi.org/10.1016/0038-0717(95)00102-6, 1996.

Kästner, M., Miltner, A., Thiele-Bruhn, S., and Liang, C.: Microbial Necromass in Soils—Linking Microbes to Soil Processes and Carbon Turnover, Front. Environ. Sci., 9, 756378, https://doi.org/10.3389/fenvs.2021.756378, 2021.

Keeling, C. D.: The concentration and isotopic abundances of atmospheric carbon dioxide in rural areas, Geochim. Cosmochim. Acta, 13, 322–334, 1958.

Keiluweit, M., Wanzek, T., Kleber, M., Nico, P., and Fendorf, S.: Anaerobic microsites have an unaccounted role in soil carbon stabilization, Nat. Commun., 8, https://doi.org/10.1038/s41467-017-01406-6, 2017.

Kögel-Knabner, I., Guggenberger, G., Kleber, M., Kandeler, E., Kalbitz, K., Scheu, S., Eusterhues, K., and Leinweber, P.: Organo-mineral associations in temperate soils: Integrating biology, mineralogy, and organic matter chemistry, J. Plant Nutr. Soil Sci., 171, 61–82, https://doi.org/10.1002/jpln.200700048, 2008.

Kuka, K., Franko, U., and Rühlmann, J.: Modelling the impact of pore space distribution on carbon turnover, Ecol. Model., 208, 295–306, https://doi.org/10.1016/j.ecolmodel.2007.06.002, 2007.

Kuzyakov, Y. and Domanski, G.: Carbon input by plants into the soil. Review, J. Plant Nutr. Soil Sci., 163, 421–431, https://doi.org/10.1002/1522-2624(200008)163:4<421::AID-JPLN421>3.0.CO;2-R, 2000.

Lehmann, J., Hansel, C. M., Kaiser, C., Kleber, M., Maher, K., Manzoni, S., Nunan, N., Reichstein, M., Schimel, J. P., Torn, M. S., Wieder, W. R., and Kögel-Knabner, I.: Persistence of soil organic carbon caused by functional complexity, Nat. Geosci., 13, 529–534, https://doi.org/10.1038/s41561-020-0612-3, 2020.

Li, C., Frolking, S., Crocker, G. J., Grace, P. R., Klír, J., Körchens, M., and Poulton, P. R.: Simulating trends in soil organic carbon in long-term experiments using the DNDC model, Geoderma, 81, 45–60, 1997.

https://doi.org/10.5194/egusphere-2024-107
Preprint. Discussion started: 30 January 2024

Liang, C., Amelung, W., Lehmann, J., and Kästner, M.: Quantitative assessment of microbial necromass contribution to soil organic matter, Glob. Change Biol., 25, 3578–3590, https://doi.org/10.1111/gcb.14781, 2019.

Liu, X.-J. A., Sun, J., Mau, R. L., Finley, B. K., Compson, Z. G., Van Gestel, N., Brown, J. R., Schwartz, E., Dijkstra, P., and Hungate, B. A.: Labile carbon input determines the direction and magnitude of the priming effect, Appl. Soil Ecol., 109, 7–13, https://doi.org/10.1016/j.apsoil.2016.10.002, 2017.

Mendoza, O., De Neve, S., Deroo, H., Li, H., and Sleutel, S.: Do interactions between application rate and native soil organic matter content determine the degradation of exogenous organic carbon?, Soil Biol. Biochem., 164, 108473, https://doi.org/10.1016/j.soilbio.2021.108473, 2022a.

Mendoza, O., De Neve, S., Deroo, H., and Sleutel, S.: Mineralisation of ryegrass and soil organic matter as affected by ryegrass application doses and changes in soil structure, Biol. Fertil. Soils, 58, 679–691, https://doi.org/10.1007/s00374-022-01654-9, 2022b.

Paustian, K., Andren, O., Janzen, H., Lal, R., Smith, P., Tian, G., Tiessen, H., Van Noordwijk, M., and Woomer, P.: Agricultural soils as a sink to mitigate CO2 emissions, Soil Use Manag., 13, 230–244, 1997.

Paustian, K., Larson, E., Kent, J., Marx, E., and Swan, A.: Soil C Sequestration as a Biological Negative Emission Strategy, Front. Clim., 1, 8, https://doi.org/10.3389/fclim.2019.00008, 2019.

Powlson, D. S., Smith, P., and Smith, J. U.: Evaluation of soil organic matter models: using existing long-term datasets, Springer Science & Business Media, 2013.

Reddy, K. R. and DeLaune, R. D.: Biogeochemistry of wetlands: science and applications, CRC Press, Boca Raton, FL., 2008.

Schjønning, P., Thomsen, I. K., Møberg, J. P., de Jonge, H., Kristensen, K., and Christensen, B. T.: Turnover of organic matter in differently textured soils: I. Physical characteristics of structurally disturbed and intact soils, Geoderma, 89, 177–198, 1999.

Schneckenberger, K., Demin, D., Stahr, K., and Kuzyakov, Y.: Microbial utilization and mineralization of [14C]glucose added in six orders of concentration to soil, Soil Biol. Biochem., 40, 1981–1988, https://doi.org/10.1016/j.soilbio.2008.02.020, 2008.

Shahbaz, M., Kuzyakov, Y., and Heitkamp, F.: Decrease of soil organic matter stabilization with increasing inputs: Mechanisms and controls, Geoderma, 304, 76–82, https://doi.org/10.1016/j.geoderma.2016.05.019, 2017a.

Shahbaz, M., Kuzyakov, Y., Sanaullah, M., Heitkamp, F., Zelenev, V., Kumar, A., and Blagodatskaya, E.: Microbial decomposition of soil organic matter is mediated by quality and quantity of crop residues: mechanisms and thresholds, Biol. Fertil. Soils, 53, 287–301, https://doi.org/10.1007/s00374-016-1174-9, 2017b.

Smith, P., Soussana, J., Angers, D., Schipper, L., Chenu, C., Rasse, D. P., Batjes, N. H., Van Egmond, F., McNeill, S., Kuhnert, M., Arias-Navarro, C., Olesen, J. E., Chirinda, N., Fornara, D., Wollenberg, E., Álvaro-Fuentes, J., Sanz-Cobena, A., and Klumpp, K.: How to measure, report and verify soil carbon change to realize the potential of soil carbon sequestration for atmospheric greenhouse gas removal, Glob. Change Biol., 26, 219–241, https://doi.org/10.1111/gcb.14815, 2020.

Vance, E. D., Brookes, P. C., and Jenkinson, D. S.: An extraction method for measuring soil microbial biomass C, Soil Biol. Biochem., 19, 703–707, https://doi.org/10.1016/0038-0717(87)90052-6, 1987.

Xiao, C., Guenet, B., Zhou, Y., Su, J., and Janssens, I. A.: Priming of soil organic matter decomposition scales linearly with microbial biomass response to litter input in steppe vegetation, Oikos, 124, 649–657, https://doi.org/10.1111/oik.01728, 2015.

https://doi.org/10.5194/egusphere-2024-107
Preprint. Discussion started: 30 January 2024

Zomer, R. J., Bossio, D. A., Sommer, R., and Verchot, L. V.: Global Sequestration Potential of Increased Organic Carbon in Cropland Soils, Sci. Rep., 7, 15554, https://doi.org/10.1038/s41598-017-15794-8, 2017.

585